Optical properties of DNA-hosted silver clusters

Markesevic, N.

CHAPTER 5

Lifetime measurements of the DNA-hosted (Ag:DNAs) silver clusters

In this Chapter, time-resolved optical measurements on individual and collections of Ag:DNAs immobilized in poly(vinyl alcohol) (PVA) are presented. Two cases of Ag:DNA collections are considered. The first case is simply a high density of individual Ag:DNAs that might form small aggregates. The second case makes use of a DNA nanotube scaffold onto which Ag:DNA emitters can be attached with a sub 10 nm spacing. We investigate the effect of the density of emitters on the optical lifetime of the emitters. Single emitters show single exponential decay when excited with a pulsed laser. The lifetime value slightly changes for longer exposure periods. A collection of emitters excited at the same time shows a double exponential decay. The longer lifetime corresponds to the value of single emitters and the shorter lifetimes are attributed to the interaction between nearby emitters. The interaction provides addition energy decay channels leading to a shorter optical lifetime. Emitters organized on the DNA tubes also show a double exponential decay, with the longer lifetimes corresponding to the values of single emitters and shorter lifetimes again indicating the interaction between the emitters. Comparing the case of the random collection of individual emitters and the case of the ordered array of emitters on a tube, we find that the weight of the shorter lifetime component significantly increases for the ordered array.

5.1 Introduction

The advances in DNA nanotechnology have completely changed the perspective of the possibilities in the manipulation and organization of matter at the nanometer scale [23, 24]. The organization of organic dyes [25, 26] and plasmonic particles [26, 78, 96, 97] as well as the dynamic change of the DNA structures [28, 97] are only some of the achievements in the field. DNA scaffolds also enabled the formation of 'hybrid' systems stabilizing plasmonic particles and organic dyes [96, 97] in special geometric configurations. This kind of constructs helps in understanding the behavior of organic dyes in plasmonic cavities, with further applications in chemistry and physics.

The formation of elaborate DNA structures relies on the complementarity of the DNA base binding (Watson-Crick pairing). The rest of the process focuses on a careful salt concentration adjusting which provides the stability of the construct. Furthermore, these constructs may have sticky ends, single strands of DNA, which typically protrude from the structure in order to perform various functions, such as connecting to other DNA constructs or stabilization of the particles, again based on the principle of complementarity.

In this Chapter, we are particularly interested in structurally and spectrally pure Ag:DNAs [53, 76], formed separately from the DNA tubes, unlike the approach in the previous chapter. Namely, the Ag:DNAs are spectrally impure and more than 90 % of the DNA strands stabilize non-fluorescent products. Working with spectrally pure emitters facilitates the process of the examination of the interactions between the emitters. Therefore, in this research we use the emitters purified with high performance liquid chromatography (HPLC). Furthermore, the emitters are designed to have sticky ends (linkers) which will enable them to connect to DNA scaffolds with complementary sticky ends (dockers).

To form the scaffolds with dockers, the procedure published by Yin et al. [34] was slightly modified appending the U6 strand with the docker, which will protrude outside the DNA construct. Finally, the purified emitters and the tubes are brought together and the attachment took place leading to the decoration of the DNA tubes with Ag:DNAs.

The fluorescence behavior of organic dyes strongly depends on their environment. For example, a fluoresncent lifetime values of FAM and Cy3 are

3.53 ns and 1.3 ns, respectively, but in the vicinity of a gold nanoparticle (d=1.5nm), the values change significantly [103]. Also, Busson and coworkers demonstrated the decay rate enhancements of 2 orders of magnitude for ATTO 647N coupled to the bright mode of plasmonic cavity [104].

The interaction between Ag:DNAs has already been discussed previously, where we used spectrally matched donors and acceptors to detect Förster energy transfer [80]. A different way to show the interaction of the emitters positioned in close proximity of one another is to measure their fluorescence lifetime, similarly to the cases where the organic dyes are positioned in the vicinity of metal particles [103, 104]. Shortening of the fluorescence lifetime can be caused by a collective emission of resonantly interactions or quenching of emission due to energy transfer to non-radiative Ag clusters. Our main aim is to examine the interactions of the DNA-hosted silver clusters precisely positioned on the DNA scaffolds.

Single DNA emitters show single exponential decay as discussed by Hooley et al. [105]. This value changes slightly during the exposure period. The lifetimes of the single emitters should be, in principle, significantly different from the lifetimes obtained from interacting emitters. In general, if a mixture of the individual emitters and collection of interacting emitters is produced, we would expect to see (at least) two lifetime components, one which corresponds to the lifetime of single emitters, and another shorter, as a consequence of the interaction between the emitters.

5.2 Synthesis procedure

The samples are provided by the group of professor Elisabeth Gwinn at University of California, Santa Barbara and the detailed synthesis procedure is given in reference [35]. The oligonucleotide sequences used in this study are presented in the Table 5.1 Single stranded DNA has two roles: to enable a formation of the stable cluster and to have an appended linker sequence. The later role will enable an efficient attachment to the DNA scaffolds via complementary single stranded 'docker' sequences. Final concentrations for synthesizing Ag:DNAs were 15.0 μM DNA, 188 μM $AgNO_3$, and 93.8 μM $NaBH_4$ .The fluorescent emitters were HPLC purified as explained in references [19, 35].

The 10-helix DNA nanotubes are chosen as scaffolds for Ag:DNAs (see

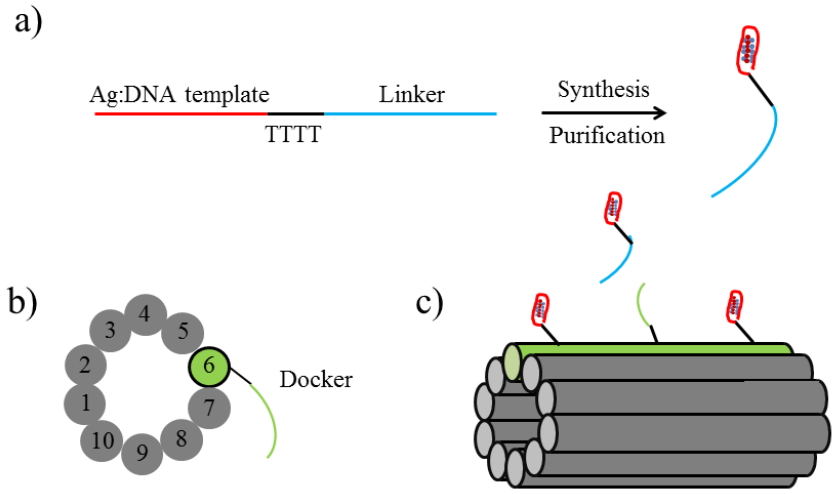

Figure 5.1: Schematic representation of the attachment of Ag:DNAs to the 10-helix DNA nanotubes [35]. a) A red-labeled part of the strand stabilizes silver cluster, which is separated by four thymines (TTTT) from the linker part which does not participate and does not influence the formation of the cluster. b) A cross-section of the DNA tube with a modified U6 strand which is appended by the docker strand. c) A schematic representation of the Ag:DNA attachment to the DNA tube. A single-stranded linker (blue) of the strand which carries silver cluster and a single-stranded docker (green) which is a part of the DNA tubes are complementary strands and thus enables the attachment.

	Name	DNA sequence (5′-3′)
1	U1	GGC-GAT-TAG-GAC-GCT-AAG-CCA-CCT-TTA-GAT-CCT-GTA-TCT-GGT
2	U2	GGA-TCT-AAA-GGA-CCA-GAT-ACA-CCA-CTC-TTC-CTG-ACA-TCT-TGT
3	U3	GGA-AGA-GTG-GAC-AAG-ATG-TCA-CCG-TGA-GAA-CCT-GCA-ATG-CGT
4	U4	GGT-TCT-CAC-GGA-CGC-ATT-GCA-CCG-CAC-GAC-CTG-TTC-GAC-AGT
5	U5	GGT-CGT-GCG-GAC-TGT-CGA-ACA-CCA-ACG-ATG-CCT-GAT-AGA-AGT
6	U6	GGC-ATC-GTT-GGA-CTT-CTA-TCA-ATG-CAC-CTC-CAG-CTT-TGA-ATG
7	U7	GGA-GGT-GCA-TCA-TTC-AAA-GCT-AAC-GGT-AAC-TAT-GAC-TTG-GGA
8	U8	TAG-TTA-CCG-TTT-CCC-AAG-TCA-AAC-ACT-AGA-CAC-ATG-CTC-CTA
9	U9	GTC-TAG-TGT-TTA-GGA-GCA-TGT-CGA-GAC-TAC-ACC-CTT-GCC-ACC
10	T10	GTG-TAG-TCT-CGG-GTG-GCA-AGG-CCT-AAT-CGC-CTG-GCT-TAG-CGT
11	U6-docker	GGC-ATC-GTT-GGA-CTT-CTA-TCA-ATG-CAC-CTC-CAG-CTT-TGA-ATG-TTT-TAT-TTA-TAC-AAC-GGA
12	Ag15-DNA host	CAC-CGC-TTT-TGC-CTT-TTG-GGG-ACG-GAT-ATT-TTT-CCG-TTG-TAT-AAA-T

Table 5.1: DNA sequences [35]. DNA oligomers used for the construction of 10-helix DNA tubes (1-10), tubes with dockers (1-11) and Ag:DNA host strands (12). Ag:DNA host strands consist of templates which stabilizes silver cluster, TTTT spacers and a linker which will enable binding to the DNA tubes.

Figure 5.1) because their architecture allows a formation of single-stranded DNA docker extrusions at separations of 7.1 nm along, but also due to the fact that their length of ~ 10 μm allows visualization by fluorescence microscopy. Using a similar approach as previously published for gold nanoparticles [36],

one of the ten 42-base long oligomers that form tubes (3'-end of U6 in our case) was appended to the docker sequence which is complementary to the linkers. The oligomers were mixed in 0.2 mL PCR tubes, each oligomer at a final concentration of 1.4 μM, in 40 mM ammonium acetate and 12 mM magnesium acetate to a final volume of 50 μL. After the annealing process using a Mastercycler personal (Eppendorf), the tubes were stored at 4°. For nanotubes with 50 % docker coverage, U6 and U6-docker site oligomers were mixed at 1:1 ratio to a total final concentration of 1.4 μM.

In order to attach Ag:DNAs to the annealed nanotubes, the Ag:DNAs were added at 5 time greater concentration than the concentration of docker sites appended to nanotubes. Buffer concentration was maintained (40 mM ammonium acetate and 12 mM magnesium acetate) to preserve the stability of the nanotubes.

5.3 Experimental section

Figure 5.2 is a schematic overview of the experimental setup. A pulsed laser (639 nm) driven at 20 MHz repetition rate was controlled by PDL 800-B (PicoQuant) in order to excite the fluorescent emitters. Linearly polarized laser light was transmitted through a narrow band filter (LD01-640/8-25, Semrock) and coupled into a single-mode optical fiber (OZ Optics). After reflection from a dichroic mirror (ZT640 RDC, Chroma) the beam was sent through an infinity-corrected high numerical aperture (NA) oil immersion objective (1.4 NA, 100X oil, Zeiss). The sample immobilized on a glass substrate was mounted on a scanning stage which was controlled by nanopositioning piezo elements (P517.3CD, Physik Instrumente). The same objective was used to collect emitted light which was further transmitted through the dichroic mirror and filtered through an emission filter (ET655LP, Chroma) to reject the reflected and scattered light. In order to remove the out-of-focus signal, the emission light was then focused onto a 75 μm pinhole and finally on the single-photon counting module (SPCM-AQR-14, Perkin Elmer). A photon counting PC-board (TimeHaro 200, PicoQuant) in the time-tagged time-resolved mode was used for data acquisition. For the controle of hardware and data acquisition as well as data processing, we used software SymPhoTime (PicoQuant).

Emitters immobilized in PVA are first detected in a raster scan. After

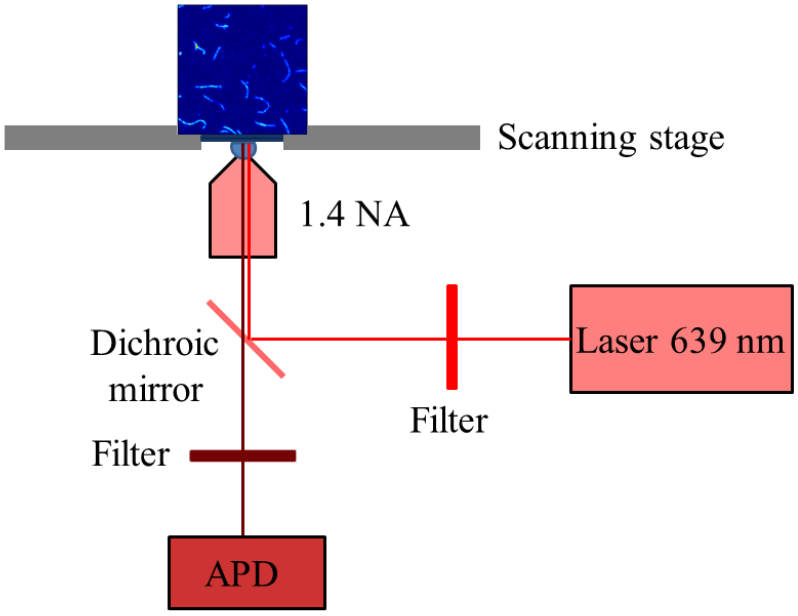

Figure 5.2: Experimental setup. Emitters immobilized in PVA on the glass slide are mounted on the scanning stage in the focus of an oil-immersion objective (1.4 NA). The laser light (excitation wavelength: 639 nm, repetition rate: 20 MHz) is transmitted through the narrow-band filter and reflected from the dichroic through the objective. The emission light is collected by the same objective, transmitted through the dichroic mirror and the emission filter, and focused on the single-photon counting module (APD).

acquiring an image, it is further possible to examine the points of interest by focusing laser light (0.5 μW) and collecting photons for 60 s. From the photon statistics we can extract information about blinking and lifetime of the emitter(s). The time-traces typically show one or several blinking steps depending on the number of emitters in the focus. To estimate lifetimes, we fit a single exponential decay function or a double exponential depending on the obtained experimental results. The functions are given in the Equations 5.1 and 5.2:

$$f = A_0 + A_1 \cdot exp(-t/\tau), \tag{5.1}$$

where A_0 represents a 'local' background, A_1 is an amplitude and τ corresponding lifetime.

$$f = A_0 + A_1 \cdot exp(-t/\tau_1) + A_2 \cdot exp(-t/\tau_2), \tag{5.2}$$

where A_0 represents a 'local' background, A_1 and A_2 are the amplitudes and τ_1 and τ_2 are longer and shorter lifetimes, respectively.

To determine the background, we use a linear fit (constant function) in the time segment before the pulse. We perform a tail-fitting routine neglecting all photons which come in the time domain of the instrument response function (IRF). To justify this, it is important to mention that the lifetimes of the Ag:DNAs are of the order of few nanoseconds, which is significantly longer than the laser pulse width of 80 ps.

5.4 Results for single emitters

Firstly, we present measurements performed on singe Ag:DNA emitters immobilized in PVA. The fluorescence image of the emitters immobilized in PVA is presented in Figure 5.3 a. By focusing light on an arbitrary chosen bright spot, we select single emitters according to the recorded time trace. Namely, the time traces that show one step blinking/bleaching are considered to belong to single emitters. In Figure 5.3 b, we present one such time trace, where it can clearly be seen that the emitter switches on and off during the excitation process. To estimate lifetimes, we split the time trace into 20 equal intervals and determine the lifetimes on each of the interval. In Figure 5.3 c, we present the average fluorescence lifetime on the interval from 24 to 27 s (red segment in Figure 5.3 b). In Figure 5.3 c the black solid line represents the instrument response functions (IRF), the red curve represents the fluorescence decay curve, and the blue line is a single exponential decay fit.

In Figure 5.4, we present the average lifetime of the emitter. The lifetime changes slightly during the process and the average value is 3.6 ± 0.1 ns. However between 39 and 42 s, we cannot estimate lifetime, because the emitter is in the off-state. In this case, the lifetime value increases during the excitation process, which is not a general trend for other emitters. We have performed similar measurements on other emitters and the average lifetime value spans between 3.2 and 3.6 ns.

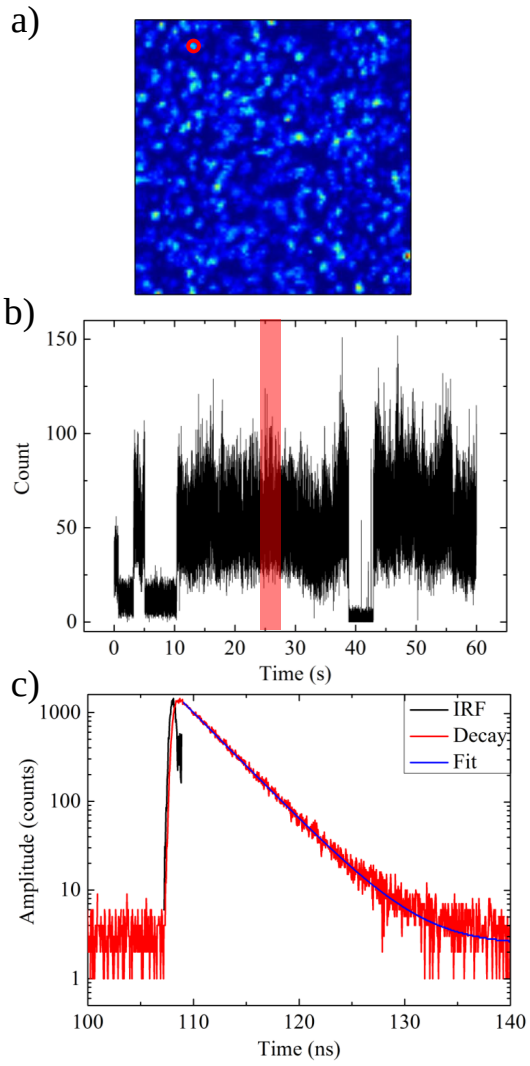

[h!]

Figure 5.3: Fluorescence properties of single emitters. a) Fluorescence image of emitters immobilized in PVA (imaged area: 20X20 μm). The excitation spot is marked with a red circle. b) Time-trace shows an on-off state of a single emitter. We want to estimate the average lifetime of the emitter along the time trace. c) The average fluorescence lifetime of the single emitter in the interval between 24 and 27 s (red segment in b)) is 3.6 ns. The red curve represents the decay curve, the blue line represents the fit (single exponential), and the black line represents an instrument response function (IRF).

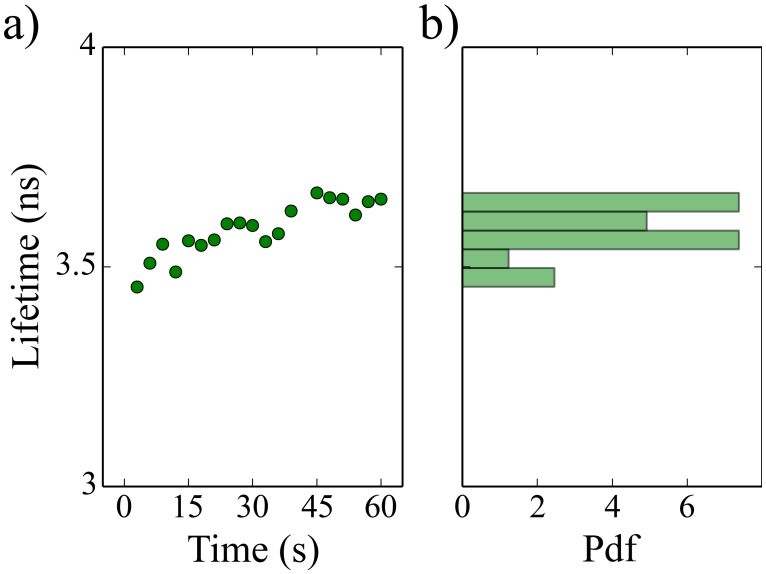

Figure 5.4: Lifetime of single emitter. a) The lifetime of a single emitter averaged every 3 s. The value increases slightly, but this can be attributed only to this emitter and does not represent a general rule. Since the emitter is in the off state the lifetime cannot be estimated in the range from 39 to 42 seconds. b) A histogram represents probability density function (PDF) of lifetime values. The average lifetime value for this emitter is 3.6 ns.

5.5 Results for multiple emitters

To examine the behavior of multiple emitters excited at the same time, we spincast the emitters dissolved in PVA with 100 times higher concentration than in the case of single emitters. A typical fluorescence image is presented in Figure 5.5 a. In Figure 5.5 b, we present the typical time-trace of the emitters excited by the pulse laser. The emitters show blinking behavior, switching on and off. For example, after 20 seconds, several of them bleached, but some recovered again. Similarly to the case of single emitters, we split the time trace into 20 intervals and estimate the average lifetimes. In this case, a single exponential decay curve does not fit to the data, but a double exponential provide a reasonable fit. In Figure 5.5 c we present the decay of the photons from the interval 45-48 s (Figure 5.5 b). This is expected, because the emitters have different orientations in space and they will have different

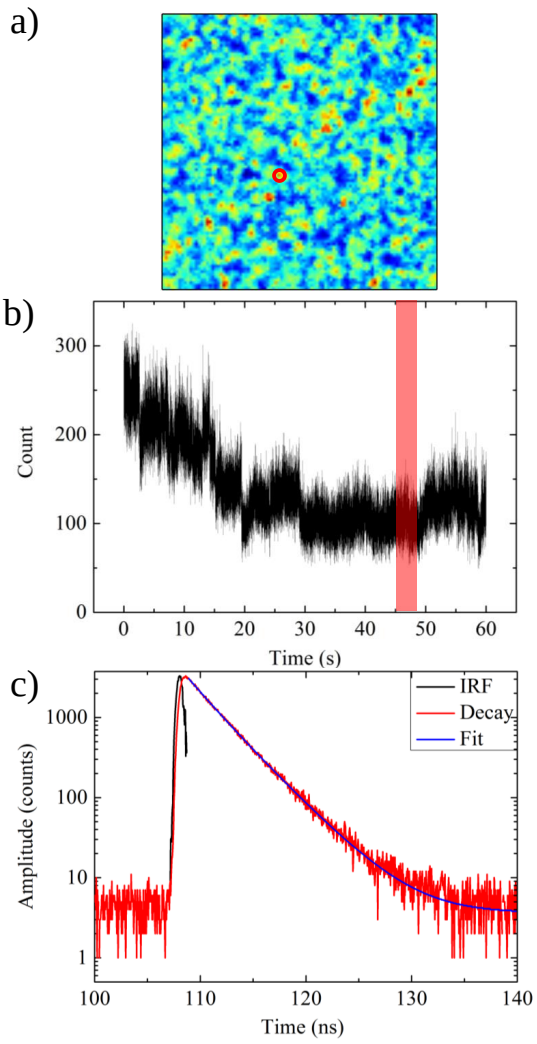

Figure 5.5: Fluorescent properties of multiple emitters. a) Fluorescence image of emitters immobilized in PVA (imaged area: 20X20 μm). The excitation spot is marked with red circle. b) Sixty-second-long time-trace shows several blinking/bleaching steps of the collection of emitters. For example, after 20 s, some of the emitters switch on again. c) To estimate the average lifetime in the interval 45-48 s (a red segment in b)) it is necessary to use double-exponential curve with lifetimes (lifetime values are 3.4 ns and 2.2 ns and the amplitude of the longer lifetime is 1.8 times larger). The red curve represents the decay, the blue curve is the double exponential function, and the black curve is the IRF.

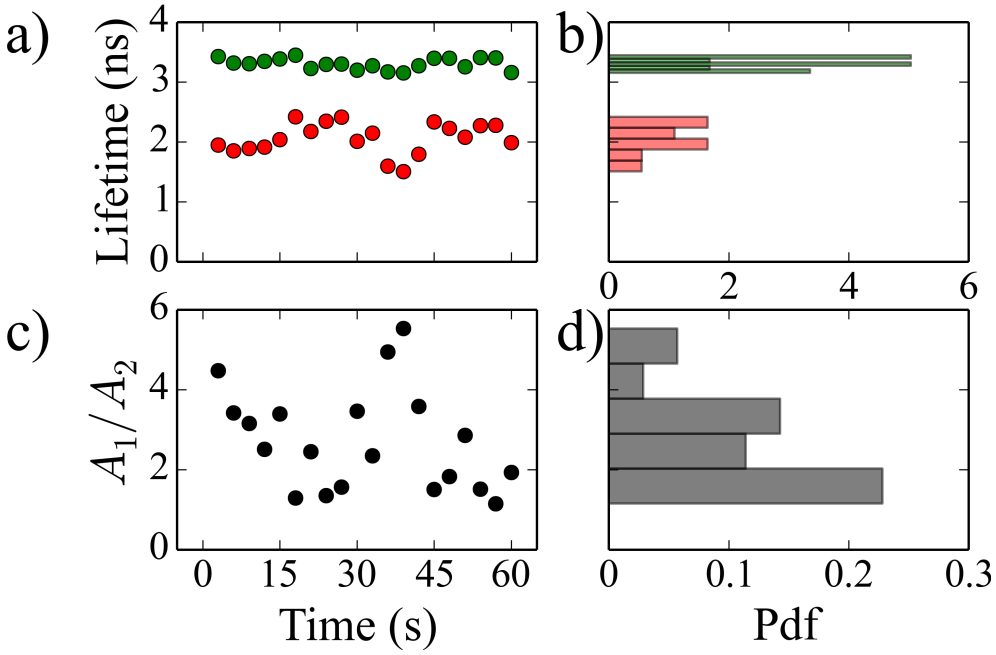

Figure 5.6: Lifetime of multiple emitters. a) The lifetime of the emitters averaged every 3 s show that the lifetimes curves can be approximated with double exponential curves. b) Probability density function (PDF) of the longer and shorter lifetime components is presented in the histogram. The longer lifetime values are centered around 3.3 $\pm$ 0.1 ns, whereas the average shorter lifetime is 2.1 $\pm$ 0.3 ns. c) A contribution of the longer and shorter lifetime components is given by the ratio of the amplitudes A_1 and A_2. d) A histogram of the amplitude ratio shows that most of the time, a shorter lifetime component has a significant contribution.

contributions. However it is possible to approximate the multi-exponential decays with double exponential.

To get better insight into the lifetime statistics along the time-trace in Figure 5.6 a we present both longer lifetimes (green circles) and shorter lifetimes (red circles). The longer lifetimes values are centered around 3.3 $\pm$ 0.1 ns, whereas the values of shorter lifetimes have an average value of 2.1 $\pm$ 0.3 ns, as presented in Figure 5.6 b. If we ascribe the shorter lifetime value to the interaction between the emitters, it seems that the shorter lifetime component is more sensitive to fluctuations than the longer, which is ascribed to the non-interacting emitters. This can be concluded from comparison of the dis-

tribution widths in Figure 5.6 b. To estimate the relative contributions of the longer and shorter lifetime components, we find the ratio between the amplitudes of the longer (A_1) and shorter lifetime (A_2) components (Figure 5.6 c). We make the following observations. First, it seems that the shorter lifetime component has a significant contribution to the exponential decay. As we can observe from the histogram in Figure 5.6 d, most of the time, the contribution is larger than 25 %. Second, despite the fact that the number of active emitters over time is decreasing as presented in Figure 5.5 b, the contribution of the shorter component does not decrease. It seems that the contribution of the shorter lifetime component is somewhat random, and does not depend on the number of active emitters.

5.6 Results for emitters on DNA tubes

In this section we investigate emitters organized on predetermined sites on the tubes which have 50 % or 100 % U6 strands appended with dockers which can stabilize the silver clusters. First we start with emitters on the 50 % labeled tubes. Their average mutual distance should be larger than 7.1 nm. From the fluorescence image presented in Figure 5.7 a, it seems that the emitters are distributed inhomogeneously on the tubes, which is in good correspondence with results presented in reference [35] . U6 strands with dockers are randomly interwoven in the tubes and also Ag:DNAs attach randomly, which is a reason for their non-uniform distribution. The time trace presented in the Figure 5.7 b shows that at the beginning of the process there are several emitters which blink and bleach during the acquisition process. After 25 s, most of them bleached. It is difficult to estimate the number of emitters within a diffraction limited spot due to the fact that the emitters are randomly orientated in space. The excitation efficiency and the emission intensity of each of them will be different, leading to the diverse step sizes. This is one of the reasons why the steps may have different sizes. Also, it is possible that two or more emitters switch on and off at the same time. As before, we tend to determine the average lifetimes of the emitters on the tubes. In Figure 5.7 c we present the average lifetimes estimated form the photons which arrived in the interval between 3 and 6 seconds (red segment in Figure 5.7 b). In this interval, the longer lifetime has a value of 3.6 ns and shorter lifetime 1.8 ns.

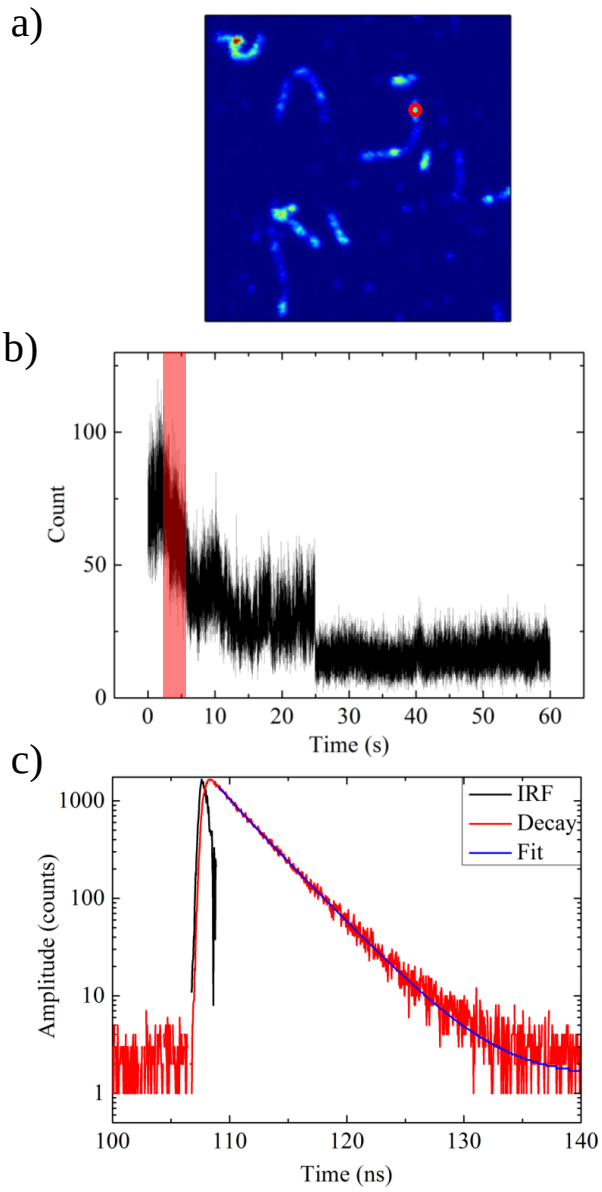

Figure 5.7: Fluorescent properties of the emitters on 50 % labeled tubes. a) Fluorescence image of the emitters stabilized on DNA tubes immobilized in PVA (imaged area: 20X20 μm). b) Time-trace of the emitters shows multiple steps indicating numerous emitters in the excitation spot (red circle in a)). c) To estimate the average lifetime of the emitters in the interval from 3 to 6 s, it is necessary to fit the double exponential curve (3.6 ns and 1.8 ns, the contribution of the longer component is 7.5 times larger).

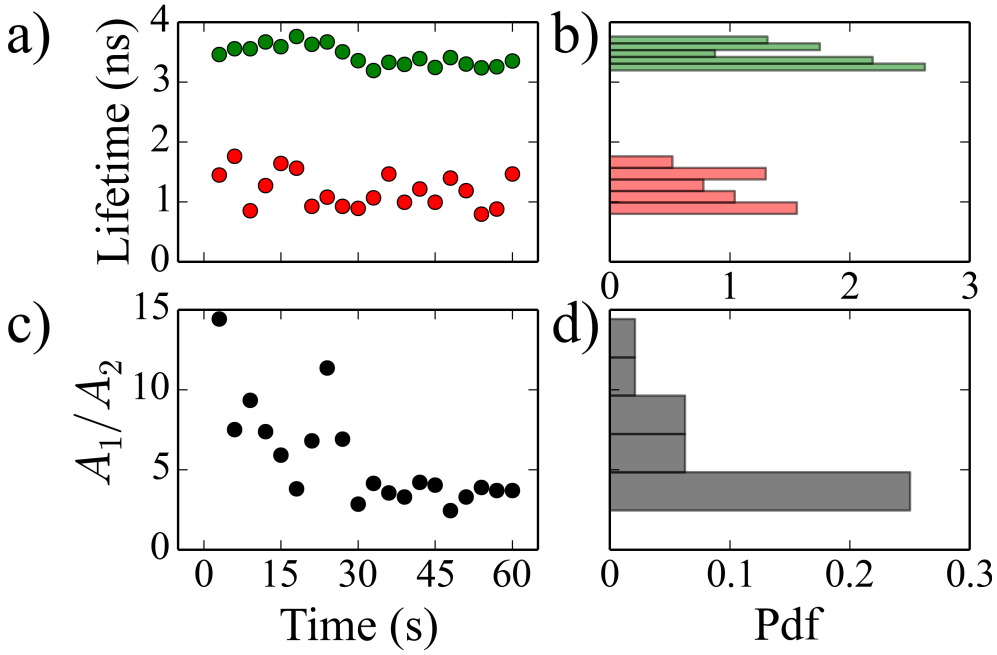

Figure 5.8: Lifetime of the emitters on 50 % labeled DNA tubes in PVA. a) The lifetime of the emitters averaged every 3 s shows that the lifetime curves can be approximated with double exponential curves. b) A histogram represents the probability density function (PDF) of the lifetime values. The average value of the longer lifetime component is 3.4 $\pm$ 0.1 ns, whereas the shorter components is around 1.2 $\pm$ 0.3 ns. c) The ratio of the amplitudes A_1 and A_2 represents the contribution of the longer and shorter lifetime components. d) A histogram of the amplitude ratio differs from the case of multiple emitters, showing that the shorter lifetime component most of the time has more than 20 % contribution in the decay.

To investigate further this process, we follow the change of the lifetimes by dividing the interval of 60 s into 20 equal intervals and estimate the average lifetime on each of those. The results shown in Figure 5.8 a show that on the entire interval the decay curves can be approximated with the double exponential curves. The average value of the longer lifetime is 3.4 $\pm$ 0.1 ns, and 1.2 $\pm$ 0.3 ns for the shorter lifetime. Histograms in Figure 5.8 b shows the probability density distribution (PDF) of the lifetimes. The contribution of the shorter and longer components are presented in 5.8 c through the amplitude ratio. From Figure 5.8 a and Figure 5.8 c, it seems that the blinking

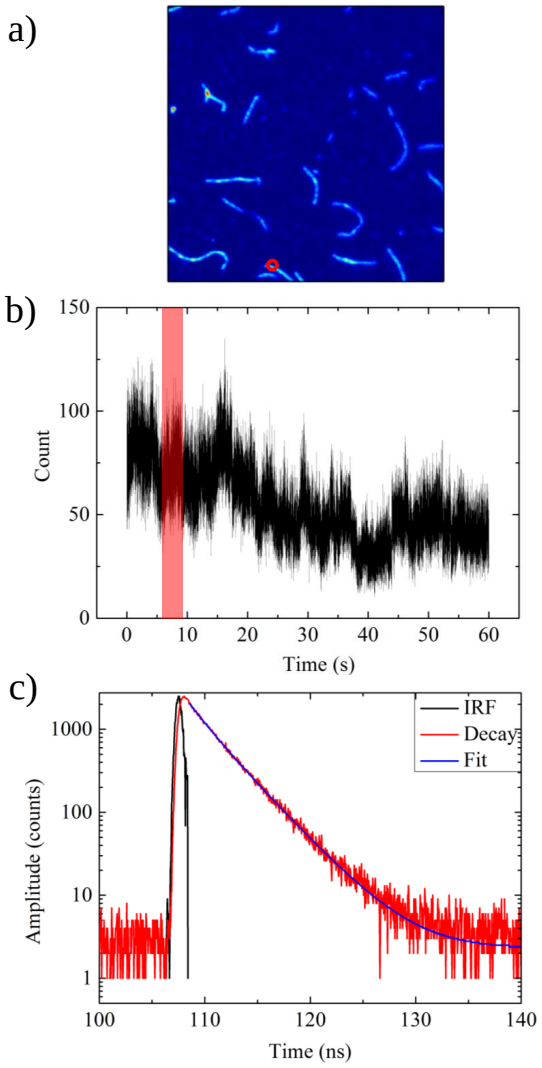

Figure 5.9: Fluorescent properties of the emitters on 100 % labeled tubes. a) Fluorescence image of the emitters stabilized on DNA tubes immobilized in PVA (imaged area: 40X40 μm). The fluorescence signal appears more uniform than in the case of 50 % labeled tubes. b) Timetrace of the emitters show multiple steps indicating numerous emitters in the excitation spot (red circle in a)). c) To estimate the average lifetime of the emitters in the interval from 6 to 9 s (red interval in b)), it is necessary to fit the double exponential curve (3.3 ns and 1.7 ns, the contribution of the longer component is 3 times larger).

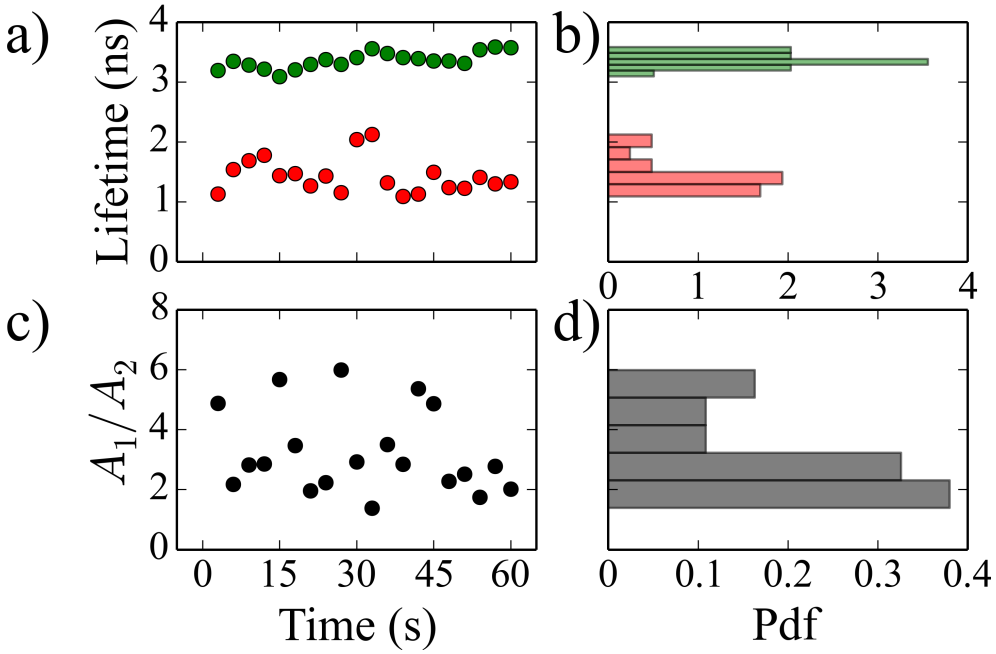

Figure 5.10: Lifetime of the emitters on 100 % labeled DNA tubes in PVA. a) The lifetime of the emitters averaged every 3 s show that the lifetime curves can be approximated with double exponential curves. b) The average value of for longer and lifetime components are 3.4 $\pm$ 0.1 ns and 1.4 $\pm$ 0.3 ns, respectively. c) The contribution of the longer and shorter lifetimes is given by the ratio of the amplitudes A_1 and A_2. d) From the histogram of the amplitude ratio, it seems that 75 % of time, the contribution of the shorter lifetime component is higher than 25 %. PDF represents probability density distribution of the ratio between the longer and shorter lifetime component.

process and the lifetime values are not related. As presented in Figure 5.8 d, it seems that half of the time, the shorter lifetime components are more than 20 % present. We note that Figure 5.8 c indicates that the shorter lifetime becomes more important after some initial period ($\sim$ 30 s). A possible explanation is that if single emitters bleach there is no optical signal left, but if one of the interacting emitters bleach there is still an optical signal remaining.

Finally, we performed similar measurements on the 100 % labeled tubes. In Figure 5.9 a one can see that the coverage of the tubes is much larger than in the case of 50 % labeled tubes. However, the intensity change is still visible

along the tubes. In Figure 5.9 b, one can see the typical time trace. As in the case of multiple emitters, the emitters blink and bleach during the excitation process as is visible by the intensity jumps. To estimate the average lifetimes during the collection time, we divide again the time trace into 20 equal intervals. The decay can be approximated with the double exponential curves presented in Figure 5.9c. The longer lifetime value is 3.3 ns and the shorter is 1.7 ns.

The lifetime values averaged over 3 s are presented in Figure 5.10 a. From the histogram presented in Figure 5.10 b, it follows that the average value of the longer lifetime is 3.4 $\pm$ 0.1 ns and that of the shorter is 1.4 $\pm$ 0.3 ns. The shorter lifetime component contributes more significantly (a factor of $\sim$ 2 more) to the intensity decay curve than in the case of the 50 % covered tubes as can be observed in Figure 5.10 c. From the PDF in Figure 5.10 d, it seems that the contribution of the shorter lifetime component in the fluorescent decay is higher than 25 % in three quarters of the exposure period.

5.7 Conclusion

In this research, we have shown that the single exponential decay functions can be used to fit the emission decay of single emitters. In order to make systems of interacting emitters, we investigate three different possibilities. The first way is to increase the concentration of Ag:DNAs which leads to the aggregation of several Ag:DNAs. In the other two cases we use self-assembled nanotubes to stabilize Ag:DNAs (tubes are covered with dockers (50 % or 100 %) which stabilize silver clusters. In all three cases several emitters are excited at the same time and the fluorescence decay can be approximated with a double exponential decay curve. The longer lifetime component corresponds to the lifetime of single emitters while the shorter lifetime is ascribed to the interaction between nearby Ag:DNAs. If we deal with the emitters attached to the 50 % labeled tubes, it seems that the appearance of two lifetimes is somewhat similar to the case of multiple emitters, except that the shorter lifetimes are typically shorter (1.2 $\pm$ 0.3 ns) than in the case of several emitters randomly distributed in the diffraction limited spot (2.1 $\pm$ 0.3 ns). For the 100 % labeled tubes, we see the reduction of the shorter lifetime component (1.4 $\pm$ 0.3 ns) compared to the case of multiple emitters. We also observe the increase of the contribution of a shorter lifetime component in the decay com-

pared to the 50 % labeled tubes (the amplitude ratio, A_1 / A_2, is larger for 100 % labeled tubes than for the 50 % labeled tubes). This is consistent with the fact that the average distance between the emitters on the tubes is smaller in the case of 100 % labeled tubes, which increases the interaction probability.